Collegio Carlo Alberto

Pricing multivariate barrier reverse convertibles with factor-based subordinators

Marina Marena
Andrea Romeo
Patrizia Semeraro

Carlo Alberto Notebooks

Pricing multivariate barrier reverse convertibles with factor-based subordinators

Marina Marena[1] Andrea Romeo[2] and Patrizia Semeraro[3]

[1]Department of Economics and Statistics, University of Torino
[2]Department of Economics and Statistics, University of Torino, and Collegio Carlo Alberto
[3]Corresponding author: patrizia.semeraro@polito.it Department of Architecture and Design, Politecnico di Torino.

Abstract

In this paper we study factor-based subordinated Lévy processes in their VG and NIG specifications, and focus on their ability to price multivariate exotic derivatives. Different model specifications, calibrated to a dataset of multivariate Barrier Reverse Convertibles listed at the Swiss market, show diverse ability in capturing smile patterns and recovering empirical correlations. We show how the range of the correlation spanned by the model is linked to the process marginal distributions. Our analysis finds that there exists a trade-off between marginal and correlation fit. A sensitivity analysis is performed, showing how the product's characteristics and the model's features affect Multi Barrier Reverse Convertible prices. Market and model prices are analyzed, highlighting and explaining discrepancies.

1 Introduction

Multi-asset derivative pricing is still an active field of research in financial modelling, calling for multivariate stochastic models that reproduce well-known stylised facts such as skewness and excess kurtosis of marginal return distributions. In this paper we focus on a class of multivariate subordinated Lévy processes, the $\rho\alpha$ models introduced by Luciano and Semeraro (2010). Among non-Gaussian multivariate processes, Lévy models are appealing in that they preserve analytical tractability.

An interesting testing ground for multivariate models is represented by barrier reverse convertible on multiple assets, one of the most successful instruments at the Swiss market for structured financial products. The product consists specifically in a long position on a coupon bond and in a short position on a worst-of down-and-in European put option. The worst-of feature requires a pricing model that can capture downside risk and correlation between assets.

A study on a large dataset of multi barrier reverse convertible has been conducted by Wallmeier and Diethelm (2012). They considered two multivariate Lévy processes with VG marginal specification: the model introduced by Leoni and Schoutens (2008) and the αVG model by Semeraro (2008). Both models were shown to be able to capture option smile patterns, but they exhibit limitations in their potential to match empirically observed correlations. The $\rho\alpha$ models extend the αVG model, by considering different marginal specifications and improving the correlation flexibility. In particular, two marginal specifications are considered in this work: Variance Gamma (VG) and Normal Inverse Gaussian (NIG), which, being closed under convolution, allow for straightforward pricing simulation procedures.

The purpose of this paper is two-fold. Firstly, we investigate marginal distributions and correlation structure in the $\rho\alpha$ models. This analytical study shows how the range of the correlation spanned by the model is linked to the process marginal distributions. By calibrating the model, we empirically confirm a trade-off beetween marginal and correlation fit, as observed in Guillaume (2012) and Luciano et al. (2013). In particular, a joint calibration of the marginal distributions and the correlation structure is required to obtain an accurate fit to market prices.

Secondly, we examine the pricing performance of $\rho\alpha$ models with regard to barrier reverse convertibles, one of the most popular segments of the Swiss market. A sensitivity analysis quantifies the impact of model parameters on prices and allows us to assess the relative importance of dependence structure and marginal processes, given the characteristics in terms of barrier and maturity of the contract. Accordingly, the joint calibration procedure can then be fine-tuned to the specific contract's features. Market and model prices are analysed, highlighting and explaining discrepancies.

The structure of the paper is as follows: in Section 2 we describe the structure and characteristics of a typical (multi) barrier reverse convertible as well as the pricing model. Sections 3 and 4 present the theoretical multivariate model and its specifications

in terms of VG and NIG subclasses. The dataset is described in Section 5. Section 6 is devoted to model calibration. Section 7 presents a sensitivity analysis while Section 8 shows the empirical results. The final Section 9 concludes.

2 Multi Barrier Reverse Convertible: Market and Features

The Swiss market for structured financial products is one of the largest in the world, providing the opportunity to study complex financial produtcs. Very popular structured products on the Swiss market are multi barrier reverse convertibles (MBRC). Each day about 4,000 MBRC are listed on the SIX Swiss Exchange, the principal Swiss stock exchange. Among the main issuers, there are Bank Julius Bär, Bank Vontobel, Banque Cantonale Vaudoise, Credit Suisse, Leonteq Securities, Notenstein Privatbank, UBS and Zurcher Kantonalbank.

Multibarrier reverse convertible are yield enhancing products. The investor gives up the capital protection in exchange for high coupons. More specifically, a MBRC offers the investor a high coupon rate during its lifetime, whilst, according to the price evolution of a basket of underlying assets, we can have different scenarios at maturity. If none of the prices of the underlying assets has hit a downside barrier or all the final prices are above their initial fixing level, the investor will receive 100% of principal. Otherwise, the investor will receive a given number of shares of the worst performer stock. The conversion ratio is calculated such that the product of the initial fixing level of any underlying and the conversion ratio is equal to 100. The payoff is illustrated in Figure 1.

Let $\boldsymbol{S} = \{\boldsymbol{S}(t), t \geq 0\}$ be a price process with n components. Suppose that $S_j(0) = S(0) = 100$ for all $j = 1, ..., n$ (this assumption is coherent with the conversion feature explained above) and that $\boldsymbol{B} = (B_1, B_2, ..., B_n)$ is a vector of barrier levels. Let's define the two events

$$A = \{\forall t \in [0, T], \boldsymbol{S}(t) > \boldsymbol{B}\},$$
$$A^c = \{\exists t \in [0, T], \boldsymbol{S}(t) \not> \boldsymbol{B}\}.$$

Then the payoff at maturity T can be written in compact form

$$100 - 100 \left(1 - \min_j \left(\frac{S_j(T)}{S(0)}\right)\right)^+ \mathbb{1}_{\{A^c\}}. \tag{2.1}$$

From (2.1), it is easy to see that the product can be represented as a portfolio consisting of a long position in a bond and of a short position in a worst-of European put with down-and-in feature.
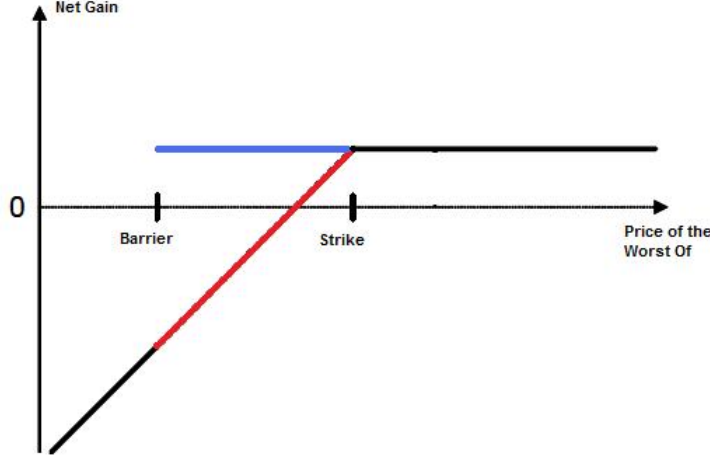
Figure 1: MBRC Payoff at Maturity. Red line: in case barrier has been triggered. Blue line: in case barrier has not been triggered.

3 Factor-based subordinated Brownian motions

This section recalls the $\rho\alpha$ models introduced in Luciano and Semeraro (2010) and their specifications with Variance Gamma (VG) and Normal Inverse Gaussian (NIG) marginal processes.

The $\rho\alpha$ models are factor-based subordinated Brownian motions constructed as the sum of two independent subordinated Brownian motions. The first has independent components, while the second is a Brownian motion with correlated marginal processes which are subordinated by a common subordinator.

Formally, let $\boldsymbol{B}$ be a n-dimensional Brownian motion with independent components and Lévy triplet $(\boldsymbol{\mu}, \Sigma, 0)$

$$\Sigma = diag(\sigma_1^2, ..., \sigma_n^2) := \begin{pmatrix} \sigma_1^2 & 0... & 0 \\ 0 & \sigma_2^2.... & 0 \\ 0 & 0... & \sigma_n^2 \end{pmatrix}, \quad \boldsymbol{\mu} = (\mu_1, ..., \mu_n).$$

Let $\boldsymbol{B}^\rho$ be a correlated n-dimensional Brownian motion, with corralations ρ_{ij}, marginal drifts $\boldsymbol{\mu}^\rho = (\mu_1\alpha_1, ..., \mu_n\alpha_n)$ and diffusion matrix

$$\Sigma^\rho := \begin{pmatrix} \sigma_1^2\alpha_1 & \rho_{12}\sigma_1\sigma_2\sqrt{\alpha_1}\sqrt{\alpha_2} & \cdots & \rho_{1n}\sigma_1\sigma_n\sqrt{\alpha_1}\sqrt{\alpha_n} \\ \rho_{12}\sigma_1\sigma_2\sqrt{\alpha_1}\sqrt{\alpha_2} & \sigma_2^2\alpha_2 & \cdots & \rho_{2n}\sigma_2\sigma_n\sqrt{\alpha_2}\sqrt{\alpha_n} \\ \vdots & \vdots & \ddots & \vdots \\ \rho_{1n}\sigma_1\sigma_n\sqrt{\alpha_1}\sqrt{\alpha_n} & \rho_{2n}\sigma_2\sigma_n\sqrt{\alpha_2}\sqrt{\alpha_n} & \cdots & \sigma_n^2\alpha_n \end{pmatrix}. \qquad (3.1)$$

The $\mathbb{R}^n$-valued subordinated process $\boldsymbol{Y} = \{\boldsymbol{Y}(t), t > 0\}$ defined by

$$\boldsymbol{Y}(t) = \begin{pmatrix} B_1(X_1(t)) + B_1^\rho(Z(t)) \\ .... \\ B_n(X_n(t)) + B_n^\rho(Z(t)) \end{pmatrix}, \tag{3.2}$$

where X_j and Z are independent subordinators, independent from $\boldsymbol{B}$ and $\boldsymbol{B}^\rho$ is a factor-based subordinated Brownian motion, also indicated as $\rho\alpha$ model.

Obviously, whenever all the parameters ρ_{ij} collapse to 0 across different components, i.e. $\rho_{ij} = 0$, for $i \neq j$, $\rho_{ij} = 1$, for $i = j$, we have a version of the model in which the Brownian motions are independent. This version has been introduced in Semeraro (2008) and is named α model.

Luciano and Semeraro (2010) (Theorem 5.1) proved that each marginal return j is a Brownian motion with parameters μ_j and σ_j subordinated by the j-th marginal process $G_j(t)$ of a factor based-subordinator $\boldsymbol{G}(t)$. A multidimensional factor-based subordinator $\{\boldsymbol{G}(t), t \geq 0\}$ is defined as follows

$$\boldsymbol{G}(t) = (X_1(t) + \alpha_1 Z(t), ..., X_n(t) + \alpha_n Z(t)), \quad \alpha_j > 0, \ j = 1, ..., n,$$

where $\boldsymbol{X}(t) = \{(X_1(t), ..., X_n(t)), t \geq 0\}$ and $\{Z(t), t \geq 0\}$ are independent subordinators with zero drift, and $\boldsymbol{X}(t)$ has independent components. They represent the idiosyncratic and the common factors of trading activity. Indeed, the following equality in law holds

$$\mathcal{L}(Y_j(t)) = \mathcal{L}(\mu_j G_j(t) + \sigma_j W(G_j(t)),$$

The marginal laws of $\boldsymbol{Y}(t)$ are therefore one-dimensional subordinated Brownian motions and we can specify the parameters of $\boldsymbol{Y}(t)$ so to have VG and NIG marginal distributions. Before introducing the two specifications we discuss the correlation structure of the model. Correlations are independent of time.

$$\rho_{\boldsymbol{Y}}(i, j) = \frac{Cov(B_i^\rho, B_j^\rho)E(Z) + E(B_i^\rho)E(B_j^\rho)V(Z)}{\sqrt{V(Y_i)V(Y_j)}}$$

$$= \frac{\rho_{ij}\sigma_i\sigma_j\sqrt{\alpha_i}\sqrt{\alpha_j}E(Z) + \mu_i\mu_j\alpha_i\alpha_j V(Z)}{\sqrt{V(Y_i)V(Y_j)}},$$

The following equation shows that correlation in these models is higher than in the the α models, i.e. the submodels with independent Brownian motions:

$$\rho_{\boldsymbol{Y}}(i, j) = \frac{\rho_{ij}\sigma_i\sigma_j\sqrt{\alpha_i}\sqrt{\alpha_j}E(Z)}{\sqrt{V(Y_i)V(Y_j)}} + \rho_{\boldsymbol{Y}_\alpha}(i, j),$$

where $\rho_{\boldsymbol{Y}_\alpha}(i, j)$ are the correlations of the α models. Correlations are increasing in α_i, α_j and in particular if $\alpha_M = max_{j \in \{i, ..., n\}}\{\alpha_j\}$, it holds:

$$\rho_{\boldsymbol{Y}}(i, j) \leq \frac{\alpha_M\sigma_i\sigma_j E(Z) + \alpha_M^2\mu_i\mu_j V(Z)}{\sqrt{V(Y_i)V(Y_j)}}.$$

4

This is true in general. However the convolution conditions required to recover VG and NIG marginal distributions link the weight parameters α_j to the common subordinator parameters, thus changing the role of α_j. The following Section 4 discusses the role of α_j for each of the two model specifications with VG and NIG marginal distributions.

4 Specifications

We now specify the process $\boldsymbol{Y}$ so that it has VG and NIG marginal distributions, as in Luciano and Semeraro (2010). The different specifications are obtained using subordinators with different distributions. For each specification we introduce the notation and parameter conditions used in the practical implementation.

4.1 Variance Gamma marginal distributions

The Variance Gamma (VG) univariate process, introduced by Madan and Seneta (1990), is a real Lévy process $L_{VG} = \{L_{VG}(t), t \geq 0\}$ which can be obtained as a Brownian motion time-changed by a Gamma process $\{G(t), t \geq 0\}$. Let $\sigma > 0$ and μ be real parameters, then the process L_{VG} is defined as

$$L_{VG}(t) = \mu G(t) + \sigma B(G(t)),$$

where B is a standard Brownian motion. Its characteristic function is

$$\psi_{VG}(u) = \left(1 - iu\mu\alpha + \frac{1}{2}\sigma^2 \alpha u^2 \right)^{-\frac{t}{\alpha}}.$$

We now specify $\boldsymbol{G}$ to have Gamma marginal distributions. Let X_j and Z be distributed according to Gamma laws:

$$\mathcal{L}(X_j) = \Gamma\left(\frac{1}{\alpha_j} - a, \frac{1}{\alpha_j} \right) \quad \text{and} \quad \mathcal{L}(Z) = \Gamma(a, 1).$$

and let the parameters α_j and a satisfy the constraints $0 < \alpha_j < \frac{1}{a}$, $j = 1, ..., n$. The subordinator $\boldsymbol{G}(t)$ has marginals $\mathcal{L}(G_j) = \Gamma\left(\frac{1}{\alpha_j}, \frac{1}{\alpha_j} \right)$ and the process $\boldsymbol{Y}$ defined in (3.2) has VG marginal processes with parameters $\mu_j, \alpha_j, \sigma_j$ - denoted as $VG\left(\mu_j, \alpha_j, \sigma_j \right)$ - i.e.

$$\mathcal{L}(Y_j) = \mathcal{L}(\mu_j G_j(t) + \sigma_j W(G_j(t))).$$

We name $\boldsymbol{Y}$ a $\rho\alpha$ Variance Gamma process, shortly $\rho\alpha$VG. The $\alpha\rho$VG model has a total of $1 + 3n + \frac{n(n-1)}{2}$ parameters: one common parameter a; the marginal parameters $\mu_j, \alpha_j, \sigma_j$ and as many additional parameters as the Brownian motions correlations ρ_{ij}, $i, j = 1, ..., n$.

We now discuss the correlation structure of the VG specification. Linear correlations are:

$$\rho_{\boldsymbol{Y}}(i,j) = \frac{\left(\mu_i\alpha_i\mu_j\alpha_j + \rho_{ij}\sigma_i\sqrt{\alpha_i}\sigma_j\sqrt{\alpha_j}\right)}{\sqrt{(\sigma_i^2 + \mu_i^2\alpha_i)(\sigma_j^2 + \mu_j^2\alpha_j)}} a.$$

They are increasing in a, which satisfies the constraint

$$0 < a < \min_j \left(\frac{1}{\alpha_j}\right).$$

This provides a bound for admissible correlations, depending on $\alpha_M = max_{j\in\{1,\ldots,n\}}\{\alpha_j\}$:

$$\rho_{\boldsymbol{Y}}(i,j) < \frac{\mu_i\mu_j\alpha_i\alpha_j + \rho_{ij}\sigma_i\sigma_j\sqrt{\alpha_i}\sqrt{\alpha_j}}{\sqrt{(\sigma_i^2 + \mu_i^2\alpha_i)(\sigma_j^2 + \mu_j^2\alpha_j)}} \frac{1}{\alpha_M}.$$

Remark 1. *Suppose $\alpha_j = \alpha$ for all j (as discussed in Leoni and Schoutens (2008)). Inequality in (4.1) becomes*

$$\rho_{\boldsymbol{Y}}(i,j) < \frac{\mu_i\mu_j\alpha + \rho_{ij}\sigma_i\sigma_j}{\sqrt{(\sigma_i^2 + \mu_i^2\alpha)(\sigma_j^2 + \mu_j^2\alpha)}}.$$

It can be shown that the upper bound for $\rho_{\boldsymbol{Y}}(i,j)$ depends on α, and, in particular, it is increasing in α if

$$\alpha > \frac{\sigma_i\sigma_j(\rho_{ij}\mu_i^2\sigma_j^2 - 2\mu_i\mu_j\sigma_i\sigma_j + \rho_{ij}\mu_j^2\sigma_i^2)}{\mu_i^3\mu_j\sigma_j^2 - 2\rho_{ij}\mu_i^2\mu_j^2\sigma_i\sigma_j + \mu_i\mu_j^3\sigma_i^2}$$

and decreasing otherwise.

The parameter α_j is linked to kurtosis k_{Y_j} of process Y_j and kurtosis k_{G_j} of subordinator G_j. Furthermore, the latter is dominated by the former, being

$$k_{Y_j} = 3(1 + 2\alpha_j - 4\alpha_j\sigma_j^4(\sigma_j^2 + \alpha_j\theta_j^2)^{-2}) < 3(1 + 2\alpha_j) = k_{G_j}.$$

As a consequence, the asset with the highest α_j drives the maximum correlation achievable. This implies a trade-off between fit of marginal kurtosis and range of model admissible correlations.

If we consider the symmetric case, by setting $\mu_i = \mu_j = 0$, we get

$$\rho_{\boldsymbol{Y}}(i,j) < \rho_{ij}\sqrt{\frac{\alpha_i}{\alpha_M}}\sqrt{\frac{\alpha_j}{\alpha_M}}.$$

We notice that in this case the bound does not depend on the kurtosis level, but only on the range spanned by the kurtosis coefficients of different marginal distributions. More generally, we conclude that the upper bound for correlation coefficients crucially depends not only on the maximum kurtosis level, but also on the kurtosis range.

The VG process has a Gamma subordinator $G(t)$ which satisfy the assumption $E[G(t)] = t$, to let stochastic time go like real time in mean. We preserve this assumption for each marginal subordinator in the construction above. By so doing we impose a constraint on the subordinator parameters. Since the VG process is the only process to have this restriction we now remove this assumption to see if the trade-off between marginal kurtosis and correlation still remain.

Let $\alpha_j, \lambda_j \in \mathbb{R}^+$ and a be such that $0 < a < \lambda_j$. Let $\mathcal{L}(X_j) = \Gamma(\lambda_j - a, \frac{1}{\alpha_j})$ and $\mathcal{L}(Z) = \Gamma(a, 1)$ and assume that X_j, $j = 1, ..., n$, and Z are independent random variables, then the random vector $\boldsymbol{W}$ defined as

$$\boldsymbol{W} = (W_1, W_2, \ldots, W_n)^T = (X_1 + \alpha_1 Z, X_2 + \alpha_2 Z, \ldots, X_n + \alpha_n Z)^T,$$

satisfies $\mathcal{L}(W_j) = \Gamma(\lambda_j, \frac{1}{\alpha_j})$, $j = 1, ..., n$ and the Lévy process $\boldsymbol{G} = \{\boldsymbol{G}(t), t \geq 0\}$ associated to the distribution of $\boldsymbol{W}$,

$$\mathcal{L}(G_j(t)) = \Gamma(\lambda_j t, \frac{1}{\alpha_j}), \quad j = 1, ..., n,$$

is a multivariate subordinator with marginal Gamma distributions. Being kurtosis of G_j equal to $3\left(1 + 2\lambda_j^{-1}\right)$, parameter λ_j drives the subordinator's kurtosis. With this specification of $\boldsymbol{G}$, the process $\boldsymbol{Y}$ is of VG type with marginal processes of VG type with four parameters $(\mu_j, \sigma_j, \alpha_j, \lambda_j)$.

Return correlations become:

$$\rho_{\boldsymbol{Y}}(i, j) = \frac{\rho_{ij}\sigma_i\sigma_j\sqrt{\alpha_i}\sqrt{\alpha_j} + \mu_i\mu_j\alpha_i\alpha_j}{\sqrt{\sigma_j^2\lambda_j\alpha_j + \mu_j^2\alpha_j^2\lambda_j}\sqrt{\sigma_i^2\lambda_i\alpha_i + \mu_i^2\alpha_i^2\lambda_i}} a.$$

In this case the convolution condition implies that the bound for a is given by $a < \lambda_m$, where $\lambda_m = min_{j \in \{1, ..., n\}}\{\lambda_j\}$. The following inequality holds

$$\rho_{\boldsymbol{Y}}(i, j) < \frac{\rho_{ij}\sigma_i\sigma_j\sqrt{\alpha_i}\sqrt{\alpha_j} + \mu_i\mu_j\alpha_i\alpha_j}{\sqrt{\sigma_j^2\lambda_j\alpha_j + \mu_j^2\alpha_j^2\lambda_j}\sqrt{\sigma_i^2\lambda_i\alpha_i + \mu_i^2\alpha_i^2\lambda_i}}\lambda_m \leq \frac{\rho_{ij}\sigma_i\sigma_j\sqrt{\alpha_i}\sqrt{\alpha_j} + \mu_i\mu_j\alpha_i\alpha_j}{\sqrt{\sigma_j^2\alpha_j + \mu_j^2\alpha_j^2}\sqrt{\sigma_i^2\alpha_i + \mu_i^2\alpha_i^2}}\frac{\lambda_m}{\lambda_m^{ij}},$$

where $\lambda_m^{ij} = min\{\lambda_i, \lambda_j\}$. With these assumption, the correlation bound depends on the new parameters λ_j. The parameters λ_j play a role similar to $\frac{1}{\alpha_j}$ in the traditional VG specification. In fact they are linked to marginal kurtosis of the subordinator and the processes Y_j since

$$k_{Y_j} = 3(1 + 2\lambda_j^{-1} - \lambda_j^{-1}(1 + 2\alpha_j^2\mu_j^4\lambda_j^{-1}\left(\alpha_j\mu_j^2 + \sigma_j^2\right)^2) \leq 3(1 + 2\lambda_j^{-1}) = k_{G_j}.$$

Therefore one asset with marginal kurtosis much higher then other assets in the portfolio implies $\lambda_m << \lambda_m^{ij}$. This highlights a trade off between marginal kurtosis and model correlation: while to have high marginal kurtosis the idyiosyncratic component must have λ_j low, the correlation parameter a is bounded by the minimum λ_j. It emerges

that the trade off depends on the convolution condition, which provides a bound for the common parameter a. The bound depends on the marginal kurtosis parameters and not on the common component weights α_j. Since the trade-off between marginals and correlation still remain, we decide to use the traditional VG in the application.

4.2 Normal Inverse Gaussian marginal distributions

A NIG process with parameters $\gamma > 0$, $-\gamma < \beta < \gamma$, $\delta > 0$ is a Lévy process $L_{NIG} = \{L_{NIG}(t), t \geq 0\}$ with characteristic function

$$\psi_{NIG}(u) = \exp\left(-\delta t\left(\sqrt{\gamma^2 - (\beta + iu)^2} - \sqrt{\gamma^2 - \beta^2}\right)\right).$$

It can be constructed by subordinating a Brownian motion with an Inverse Gaussian distribution. Let

$$X_j \sim IG\left(1 - a\sqrt{\alpha_j}, \frac{1}{\sqrt{\alpha_j}}\right), \quad j = 1, ..., n \quad \text{and} \quad Z \sim IG(a, 1),$$

where

$$0 < a < \frac{1}{\sqrt{\alpha_j}}, \quad j = 1, ..., n; \tag{4.1}$$

let now $\gamma_j, \beta_j, \delta_j$ be such that

$$\gamma_j > 0, \quad -\gamma_j < \beta < \gamma_j, \quad \delta_j > 0;$$

further, let

$$\frac{1}{\sqrt{\alpha_j}} = \delta_j\sqrt{\gamma_j^2 - \beta_j^2}. \tag{4.2}$$

If we set $\mu_j = \beta_j\delta_j^2$ and $\sigma_j = \delta_j$ in (3.1) the process $\boldsymbol{Y}$ defined in (3.2) has NIG marginal processes, i.e.

$$\mathcal{L}(Y_j) = \mathcal{L}(\beta_j\delta_j^2 G_j(t) + \delta_j W(G_j(t)))$$

We name $\boldsymbol{Y}$ a $\rho\alpha$ Normal Inverse Gaussian process, shortly $\rho\alpha$NIG. Note that the process has a total of $1 + 3n + \frac{n(n-1)}{2}$ parameters: a is a common parameter; $\gamma_j, \beta_j, \delta_j$, $j = 1, ..., n$ are marginal parameters and $\rho_{ij}, i, j = 1, ..., n$, are the $\boldsymbol{B}^\rho$ correlations.

Setting $\zeta_j = \delta_j\sqrt{\gamma_j^2 - \beta_j^2}$, the linear correlations of the $\rho\alpha$NIG process are

$$\rho_{\boldsymbol{Y}}(i,j) = \frac{\beta_i\frac{\delta_i^2}{\zeta_i^2}\beta_j\frac{\delta_j^2}{\zeta_j^2} + \rho_{ij}\frac{\delta_i}{\zeta_i}\frac{\delta_j}{\zeta_j}}{\sqrt{\left(\gamma_i^2\delta_i\left(\gamma_i^2 - \beta_i^2\right)^{-\frac{3}{2}}\right)\left(\gamma_j^2\delta_j\left(\gamma_j^2 - \beta_j^2\right)^{-\frac{3}{2}}\right)}}a.$$

They are increasing in a, and, under (4.1) and (4.2), must satisfy the constraint

$$0 < a < \min_j \zeta_j.$$

8

Thus

$$\rho_{\mathbf{Y}}(i,j) < \frac{\left(\beta_i \frac{\delta_i^2}{\zeta_i^2} \beta_j \frac{\delta_j^2}{\zeta_j^2} + \rho_{ij} \frac{\delta_i}{\zeta_i} \frac{\delta_j}{\zeta_j}\right)}{\sqrt{\left(\gamma_i^2 \delta_i \left(\gamma_i^2 - \beta_i^2\right)^{-\frac{3}{2}}\right) \left(\gamma_j^2 \delta_j \left(\gamma_j^2 - \beta_j^2\right)^{-\frac{3}{2}}\right)}} \zeta_m, \qquad (4.3)$$

where $\zeta_m = \min_j \zeta_j$.

Remark 2. *Suppose $\zeta_j = \zeta$ for all j, then (4.3) becomes*

$$\rho_{\mathbf{Y}}(i,j) < \frac{\beta_i \beta_j \delta_i^2 \delta_j^2}{\gamma_i \gamma_j} + \frac{\rho_{ij} \delta_i \delta_j \zeta^2}{\gamma_i \gamma_j},$$

that is increasing in ζ.

Since $\beta^2 \leq \gamma^2$ and $\frac{1}{\sqrt{\alpha_j}} = \zeta_j$, the kurtosis of $Y_j(t)$ is bounded by the kurtosis of the subordinator G_j

$$k_{Y_j} = 3\left(1 + \frac{\gamma_j^2 + 4\beta_j^2}{\delta_j \gamma_j^2 \sqrt{\gamma_j^2 - \beta^2}}\right) \leq 3\left(1 + \frac{5}{\zeta_j}\right) = k_{G_j}.$$

As in the VG case, the asset with the highest ζ_j drives the maximum correlation achievable, implying a trade-off between fit of marginal kurtosis and range of model admissible correlations.

If we consider the symmetric case, by setting $\delta_i = \delta_j = 0$, we get

$$\rho_{\mathbf{Y}}(i,j) < \rho_{ij} \sqrt{\frac{\zeta_m}{\zeta_i}} \sqrt{\frac{\zeta_m}{\zeta_j}},$$

As in the VG model, in this case the bound does not depend on the kurtosis level, but only on the range spanned by the kurtosis coefficients of different marginal distributions. Again, we conclude that also for the NIG specification, the upper bound for the correlation coefficients crucially depends not only on the maximum kurtosis level, but also on the kurtosis range.

5   Data

As Lindauer and Seiz (2008) pointed out, in the primary market we typically observe large overpricing, while in the secondary market the overpricing tends to decrease and disappear, and other factors seem to be decisive in the valuation of the product. For this reason, in our work we use data coming from the secondary market of multi barrier reverse convertibles.

Our dataset consists of 92 MBRC traded on 10th April, 2015, with 39 different underlying baskets. The number of underlyings ranges from two to five, being the majority

of products linked to three underlyings. Product characteristics are collected from the termsheets. We only consider products whose underlyings are Swiss stocks for which Eurex options are available. For simplicity and comparability with previous works, we exclude from our dataset any MBRC product with early redemption features. Time to maturity ranges from 1 to 2 years. Issuers are Bank Julius Bär, Bank Vontobel, Banque Cantonale Vaudoise, Credit Suisse, Leonteq Securities, Notenstein Privatbank and UBS. The underlyings considered are ABB, Credit Suisse Group, Holcim, Nestlé, Novartis, C.F. Richemont, Roche Holding, Swatch, Swisscom, SwissLife, SwissRE, Syngenta, UBS and Zurich Financial Services. Barriers range from 38% to 81% of stock prices at issuance. Coupon payments are annual, semiannual or quarterly. The annual coupon rate ranges from 3.5% to 9.75% of nominal. Continuous compound dividend yields is taken from Bloomberg and refers to the implicit dividend yield coming from the put-call Parity for American options. Risk-free rates are interpolated from the interbank offered rate curve in the CHF currency. We assume a credit spread of 25 basis points for issuers whose credit spread is not available in the product's termsheet. Historical correlations are computed on daily log returns over the previous year.

6 Calibration

Define an $n-$dimensional price process, $\boldsymbol{S} = \{\boldsymbol{S}(t),\, t \geq 0\}$, by

$$\boldsymbol{S}(t) = \boldsymbol{S}(0) \exp(\boldsymbol{c}t + \boldsymbol{Y}(t)),\, \boldsymbol{c} \in \mathbb{R}^n,$$

where $\boldsymbol{c}$ is the compensator and $\boldsymbol{Y}(t)$ is one of the Lévy specifications introduced above.

Ideally, factor-based Lévy processes should be calibrated to the market prices of MBRCs. However, since closed form pricing formulas are unlikely to be available for multi-asset exotic derivatives, this is not a feasible approach in practice. Therefore, we calibrate the correlation structure to historical correlations, as in Luciano and Schoutens (2006) and Leoni and Schoutens (2008).

The $\rho\alpha$ models allow for a two-step calibration. Firstly, we fit marginal parameters to the univariate volatility surfaces of each relevant underlying, and, secondly, we fit the common parameters to the sample correlations of the underlying basket. Although this procedure is very appealing, the bound on the common parameter a can restrict the admissible correlation range for the VG and NIG specifications. Therefore, in the spirit of Guillaume (2012), we introduce a joint calibration procedure for each basket of underlyings to enhance goodness-of-fit of the correlation structure.

6.1 Two-step calibration procedure

Firstly, marginal calibration is performed on Eurex settlement data, matching model and market put option prices. We consider only at-the-money and out-of-the-money

options with maturity between 10 days and 2 years, price greater than 0.1 CHF and open interest greater than 50, in order to have reliable data. To account for the American style of Eurex stock options, we apply the FST method proposed in Jackson et al. (2008). Calibration is achieved by minimisation of the Root Mean Square Error (RMSE) between model and market prices

$$RMSE = \sqrt{\frac{1}{N} \sum_{i=1}^{N} (P_{mkt} - P_{model})^2}.$$

Another suitable choice could be the Average Relative Percentage Error (ARPE)[1]. Secondly, we calibrate the dependence structure for each basket of underlyings by minimising the root-mean-squared error between the empirical and the $\rho\alpha$-model return correlations. This yields an estimate of the common parameter a and the Brownian correlations ρ_{ij} of the basket.

Table 1 shows the calibrated marginal parameters for each model. As one can notice, VG and NIG provide reduced errors with respect to the multivariate Gaussian model (G), both in terms of RMSE and ARPE. This is due to the ability of VG and NIG models to capture skewness and excess kurtosis, yielding a better smile-replication. However, the correlation error for both $\rho\alpha$-models is significant. The average RMSE is 0.348 in the VG specification and 0.487 in the NIG one. This result empirically supports the link between marginal processes and correlation structure of the multivariate process discussed in Section 4. For both model specifications, the bound on the pairwise correlation depends on the marginal kurtosis of the subordinators, obtained in the first calibration step.

6.2   Joint calibration procedure

In this section, we introduce a joint calibration procedure. Setting a given tolerance on the maximum absolute error in matching asset correlations, we fit all option surfaces together. In particular, for each basket of n underlyings, we numerically solve the problem:

$$\min_{\{\boldsymbol{\theta}, a, \boldsymbol{\rho}\}} \quad \sum_{i=1}^{n} RMSE_i$$
$$\text{s.t.} \quad \max |\rho_{\boldsymbol{Y}}^{emp}(j,k) - \rho_{\boldsymbol{Y}}(j,k)| \leq \epsilon, \; j \neq k$$

where $\boldsymbol{\theta}$ is the vector of all marginal parameters, $\boldsymbol{\rho} = \{\rho_{ij}, \, i = 1, \ldots n, \, j = 2, \ldots n\}$ are the correlation coefficients between the Brownian components collected in $\boldsymbol{B}^\rho$ and $\rho_{\boldsymbol{Y}}^{emp}(i,j)$ and $\rho_{\boldsymbol{Y}}(i,j)$ are the sample and model return correlations, respectively. The threshold ϵ represents the maximum acceptable level of correlation errors. Setting ϵ small (e.g., 0.01 or 0.05) ensures an almost perfect replication of the correlation structure, but larger errors in the calibration of the marginal distributions can arise. The

---

[1]$ARPE = \frac{1}{N} \sum_{i=1}^{N} \frac{|P_{mkt} - P_{model}|}{P_{mkt}}$

relative importance of marginal versus correlation fit can then be fine-tuned through the threshold ϵ. Tables 2 and 3 show the ranges of calibrated marginal parameters in the $\rho\alpha$-model specifications. The joint calibration procedure yields an average RMSE (ARPE) of 0.347 (16.77%) in VG case and an average RMSE (ARPE) of 0.467 (18.36%) in the NIG case. Marginal fit slightly worsen in the joint calibration with respect to the two-step procedure. However, the error in the correlation structure is significantly reduced. By setting $\epsilon = 10\%$, on the correlation fit we observe an average RMSE (MAE) of 0.073 (7.90%) in the VG case and an average RMSE (MAE) of 0.0078 (0.71%) in the NIG case. Interestingly, the NIG correlation fit is very good. Only for one basket out of 39 the constraint is binding at 10%. Nevertheless, while the numerical optimization procedure is straighforward in the VG specification, depending the kurtosis of the subordinators on parameters α_j only, in the NIG case, the bound depends on $\zeta_j = \delta_j \sqrt{\gamma_j^2 - \beta_j^2}$, i.e. on the interaction of all marginal parameters. How marginal parameters interplay in the multivariate process is examined in more detail in the next section.

7   Sensitivity Analysis

In this section we perform a sensitivity analysis, examining how model parameters affect the value of MBRC products. We consider a MBRC product with two underlyings and typical features: barrier levels are set to 70% of the price of each underlying at issuance, risk-free rate is 0.25%, credit-spread is 42 basis points and dividend-yield is 0. We examine two different maturities, 6 months and 1 year, and three correlation scenarios, setting the correlation coefficient to 0, 0.25 and 0.75. We define a base case, assuming the same marginal distributions for both assets, with parameters chosen consistently with the calibration results of Section 6. Different cases are obtain by either halving or doubling each parameter of the base case. Put prices are expressed as percentage of the base put price. Our analysis shows that the MBRC prices move consistently with the changes in moments of marginal distributions. We discuss below put price variations due to changes in marginal moments and correlation. While marginal moments are directly linked to marginal parameters in the VG case, this is not true for the NIG case.

   In Table 4 the VG model is considered. Marginal parameters of the base case are $\sigma = 0.230$, $\alpha = 0.377$ and $\mu = 0$ for both marginal processes. We find that the put value increases with the marginal parameter σ, which drives the variance of the marginal distribution. More specifically, if the variance of one marginal distribution increases, the put value is almost insensitive to the variance level of the other marginal, due to the worst-of feature of the product. The effect of the sign of the skewness can be read through the parameter μ. When the skewness parameter moves to negative values, the put price increases (and viceversa). The effect of marginal kurtosis on option prices depends on time to maturity. We find a direct relationship between kurtosis and option value for short maturities and an inverse relationship for long maturities, as observed

also in Wallmeier and Diethelm (2012). This can be interpreted observing Figure 2 which shows the distribution of the minimum for the two scenarios of time to maturity. When parameter α, that mainly controls kurtosis in the VG model, changes from the original level of 0.377 to $\alpha_L = \alpha/2 = 0.188$, both marginal distributions of log-returns present 6-months kurtosis of 4.1310. In the case of $\alpha_H = 2\alpha = 0.754$, 6-months kurtosis raises to 7.5238. However, this implies kurtosis levels for the 1-year distributions of 3.5655 and 5.2619. In this analysis we keep the barrier level constant for both time to maturity scenarios. This implies a shift in the distribution of the minimum of the two assets at maturity without a shift in the barrier, then the probability of hitting the barrier changes by construction. As one can notice in Figure 2, the probability of hitting the barrier is very similar in Subfigures 2a, 2c and 2e, with a slightly higher probability in the case of high kurtosis. On the contrary, in the case of 1-year maturity, the probability of hitting the barrier is higher when the kurtosis is lower (Subfigures 2b, 2d and 2f). We then observe different effects of the marginal distributions kurtosis, depending on the combination of barrier levels and maturity of the product. In particular the more the barrier level differs from the strike price, the more a direct relation between kurtosis and put value is magnified. This is because the hitting event will depend more and more on the heaviness of the left tail of the distribution. On the other hand, barriers very close to the strike price increase the probability of the hitting event in the case of more platykurtic marginal distributions. Of course, strong positive correlation implies lower put values for both short and long maturities. In our simulation, the VG model can recover a correlation level between the marginal processes of 0.75 in 9 cases out of 21 possible combinations of marginal parameters.

Table 5 shows the sensitivity results for the NIG model. The base case has marginal parameters $\gamma = 7.15$, $\beta = 0$ and $\delta = 0.378$. We notice that the option value in the case of independence between marginal processes and short maturity is very similar to the VG price, since the marginal processes present almost identical moments up to the fourth one. The moments of the NIG process cannot be moved by changing a single parameter, as in the VG setting. In the symmetric case, however, we can overcome this limitation, moving along the main diagonal of each subtable, i.e., considering processes with the same marginal distributions. In fact, we can find some parameter combination which allows to move only one moment at a time[2]. From Table 5 it emerges that the effect on the put value of a change in the marginal variances depends on the kurtosis levels of the marginal distributions. Furthermore, we observe the same relationship between kurtosis and option value as in the VG model. Similarly to μ in the VG economy, changing

---

[2]For instance, compare two different cases along the main diagonal: $(0, 2\gamma, \delta)$ and $(0, \gamma, 2\delta)$ for both marginal processes. They have different marginal variances and the same skewness and kurtosis. In fact, we have $V(Y) = \delta/(2\gamma)$ in the first case and $V(Y) = 2\delta/\gamma$ in the second one, while kurtosis is $k_Y = 3(1 + 1/2\delta\gamma)$ in both cases. The same applies with $(0, \gamma/2, \delta)$ and $(0, \gamma, \delta/2)$. To have different marginal kurtosis and the same variances and skewness, we can consider for instance $(0, 2\gamma, \delta)$, and $(0, \gamma, \delta/2)$ for both marginal processes.

the β parameter has a direct effect on the skewness of marginal distributions, with an inverse relation with respect to the worst-of put value. A correlation level of 0.75 can be recovered in 6 cases out of 21 possible combinations of marginal parameters.

Finally, Figure 3 shows the sensitivity of put prices to different correlation levels for our base case.

8   Pricing

Since no analytical pricing formula is available, we price the MBRCs of our dataset by Montecarlo simulation, with daily time step and 2^{17} paths. The time change representation of the $\rho\alpha$ models allows for a straightforward simulation procedure. Montecarlo standard errors are very little in economic sense and therefore they are not reported.

Figure 4 compares bid and ask market prices with model prices, when the the $\rho\alpha$ models are calibrated according to the joint calibration procedure. On top of that, we set the common parameters to match two correlation scenarios: maximum pairwise correlations and independence. This allows us to understand how model prices react to different correlation assumptions consistent with the marginal parameters of the joint calibration. Hence, Figure 4 shows also model prices corresponding to our correlation scenarios. MBRC are ordered depending on the time to issue, indicated on the horizontal axis of each graph. In general, the lower the time to issue, the higher the time to maturity of the product. Figure 4a, 4b and 4c show prices under the G, VG and NIG specification, respectively. The difference between G and VG prices ranges from -0.99% to 2.12%, while the difference between G and NIG prices ranges from -1.96% to 2.00%.

Model prices lie beneath bid market prices for just-issued products in all model specifications. This confirms the findings by Wallmeier and Diethelm (2008) who report an overpricing of 3.4% at issuance on their dataset of MBRCs under the multivariate Gaussian model, and a typical overpricing range of 3% to 6%. Overpricing disappears for shorter dated products, on the right hand side of figure 4. In fact, there is a slight underpricing for products with shorter time to maturity in all models.

The difference in terms of MBRC value between independent and highly positively correlated processes (i.e., the effect of correlation) is decreasing as the time to maturity decreases for all three specifications. Hence, correlation flexibility is crucial in pricing long term products. Instead, we observed a lower impact of correlation on prices of products on the left side of figure 4, which have both lower time to maturity and barrier levels. Here, the model's smile-replication ability, driven by the marginals, strongly affects prices, due to the worst-of feature of MBRCs.

The $\rho\alpha$ models with the joint calibration procedure, while preserving marginal features of pure jump processes, allow for a range of correlations sufficiently wide to explain market prices, even for just issued products. We notice that the best fit is provided by the NIG specification, which has a correlation error below 1% for most of the products.

Figure 5 provides a deeper insight on the calibration approaches, focusing on a specific basket: Nestlé, Novartis and RocheGS. The two-step calibration procedure provides a good smile replication (in terms of marginals) but underestimates correlations. This implies a sistematic overestimate of the put component of the MBRC for just issued products, corresponding to an underestimate of the price of the overall product. As soon as the role of correlation dies out, prices are replicated also by using this calibration approach.

9 Conclusions

In this work we explore the pricing performance of the VG and NIG specifications of the Lévy $\rho\alpha$ model introduced by Luciano and Semeraro (2010) for multi-asset products traded in a liquid market. We extend the study by Wallmeier and Diethelm (2012) who considered the αVG model and the model introduced in Leoni and Schoutens (2008). We empirically investigate the trade-off between marginal and correlation fit, by calibrating the model with two different approaches. In the first one, marginal parameters are calibrated on single-asset options and then common parameters are calibrated on the observed correlation matrix (two-step calibration). In the second approach, the whole set of model parameters is calibrated at the same time for each basket of underlyings (joint calibration). The second approach allows for a better fit of the correlation structure, slightly worsening the marginal fit. Not only the joint calibration improves the overall fit of the model but it also improves the pricing performance. However, both model specifications, VG and NIG, are flexible enough to outperform the G model in the smile replication, presenting the NIG the best marginal fitting performance.

We analyse critical factors affecting the price of MBRCs in terms of contract features and model parameters. Path-dependency and worst-of features strongly influence MBRC prices. In particular, the price of a MBRC decreases with its time to maturity. It depends negatively on the variance and positively on the skewness of one underlying (almost independently of the others). Correlation levels are negatively related to MBRC prices. Finally, prices depend in a nonlinear way on the kurtosis of the marginal distributions.

For just-issued products, we observe a significant overpricing regardless of the model under consideration. This stylised fact tends to decrease along the life of the product for all models.

This study shows that the class of $\rho\alpha$ models is well suited to price multi-asset derivatives. A joint calibration approach is able to exploit the trade-off between marginal distributions and correlation fit. Furthermore, under the NIG specification, we find that most market prices lie between model prices generated by assuming independence and model prices generated by assuming maximal linear dependence.

Table 1: Marginal Calibration - First Step

		G				VG					NIG		
	σ	ARPE	RMSE	σ	α	μ	ARPE	RMSE	γ	β	δ	ARPE	RMSE
ABB	0.2021	19.25%	0.0598	0.2007	0.3332	-0.1040	6.57%	0.0296	10.1334	-4.2212	0.3363	5.31%	0.0246
CS	0.2469	24.56%	0.0850	0.0867	0.0515	-1.0140	10.48%	0.0580	158.3844	-145.3693	0.6025	10.68%	0.0588
Holcim	0.2476	20.06%	0.1974	0.1061	0.0490	-1.0042	7.82%	0.1342	131.3436	-117.8635	0.6887	8.03%	0.1356
Nestlé	0.1522	41.01%	0.2753	0.1452	0.3968	-0.0922	22.24%	0.1619	2.9097	-0.2709	0.0982	12.50%	0.0939
Novartis	0.1872	36.82%	0.2207	0.1528	0.2188	-0.2190	17.47%	0.0895	20.6542	-12.4337	0.3609	15.28%	0.0815
Richemont	0.2305	29.78%	0.2275	0.2195	0.2425	-0.1772	14.91%	0.0999	9.2194	-3.5550	0.4134	12.41%	0.0826
RocheGS	0.1892	39.77%	0.5448	0.1251	0.1493	-0.3538	19.71%	0.2480	50.2539	-40.2075	0.3771	18.05%	0.2394
Swatch	0.2316	35.42%	1.1685	0.2210	0.2315	-0.1664	19.06%	0.5235	8.6782	-2.9513	0.4087	16.32%	0.4492
Swisscom	0.1802	35.19%	1.1611	0.1261	0.1906	-0.2827	15.09%	0.5507	25.7756	-17.1639	0.3417	13.16%	0.5132
SwissLife	0.2034	38.95%	0.9066	0.1889	0.3405	-0.1522	19.92%	0.4957	5.6198	-1.5276	0.2414	18.74%	0.4238
SwissRE	0.1945	36.20%	0.3190	0.2008	0.3963	-0.0471	11.55%	0.2303	3.7111	-0.2429	0.1771	11.99%	0.2092
Syngenta	0.1977	41.84%	1.1007	0.2035	0.3961	-0.0731	16.34%	0.6060	5.2121	-1.1472	0.2277	15.56%	0.5289
Zurich	0.1820	49.13%	0.8487	0.0890	0.2671	-0.3052	19.88%	0.2897	82.6999	-75.2100	0.1990	18.12%	0.2759

Table 2: Marginal calibration (joint calibration procedure). VG model

	σ		α		μ		ARPE	RMSE
	min	max	min	max	min	max	mean	mean
ABB	0.1356	0.2183	0.3716	0.7653	-0.1971	-0.0468	8.85%	0.0432
CS	0.1420	0.2299	0.3906	0.5929	-0.2777	-0.1817	15.90%	0.1115
Holcim	0.2071	0.2405	0.1193	0.2335	-0.3990	-0.1712	8.14%	0.1733
Nestlé	0.0566	0.1558	0.4181	0.8370	-0.2166	-0.0538	22.35%	0.1511
Novartis	0.0801	0.1642	0.2089	0.7053	-0.3225	-0.1056	18.88%	0.1294
Richemont	0.2322	0.2326	0.2883	0.4346	-0.1163	-0.1052	14.13%	0.1185
RocheGS	0.0049	0.1672	0.1606	0.5153	-0.4561	-0.1297	19.16%	0.3561
Swatch	0.2075	0.2280	0.1978	0.3423	-0.2044	-0.1178	19.90%	0.5353
Swisscom	0.0036	0.1189	0.2829	0.6301	-0.3007	-0.1761	13.78%	0.8118
SwissLife	0.2088	0.2091	0.5198	0.5265	-0.0912	-0.0901	24.48%	0.5747
SwissRE	0.1756	0.2076	0.4092	0.7093	-0.1429	-0.0311	14.97%	0.2374
Syngenta	0.2025	0.2162	0.3412	0.7922	-0.1192	-0.0355	18.77%	0.6216
Zurich	0.0357	0.1090	0.3794	0.6108	-0.2783	-0.1839	18.68%	0.6448

Table 3: Marginal calibration (joint calibration procedure). NIG model.

	γ		β		δ		ARPE	RMSE
	min	max	min	max	min	max	mean	mean
ABB	3.3271	5.5675	-1.2059	-0.5034	0.1467	0.2797	9.59%	0.0516
CS	3.7098	4.5953	-0.9468	-0.7751	0.1256	0.3384	33.45%	0.2482
Holcim	3.9842	9.9134	-3.3284	-0.6896	0.2938	0.5538	11.23%	0.2146
Nestlé	3.3455	4.7812	-0.9263	-0.4483	0.1039	0.1362	14.61%	0.1366
Novartis	3.6708	264.8336	-256.3779	-0.6022	0.1367	0.2736	19.98%	0.2096
Richemont	3.8377	5.0015	-1.2969	-0.6127	0.2491	0.2667	14.69%	0.1751
RocheGS	3.3124	114.1302	-104.5217	-0.5140	0.1166	0.2823	22.68%	0.6470
Swatch	3.5760	9.1174	-3.9210	-0.6229	0.2243	0.4282	22.50%	0.5870
Swisscom	3.6769	220.3856	-213.2334	-0.4735	0.1087	0.3117	13.07%	1.4213
SwissLife	3.9136	4.5566	-0.9440	-0.4700	0.1961	0.2313	20.33%	0.4807
SwissRE	3.5030	4.4791	-1.3061	-0.4064	0.1374	0.2099	15.78%	0.2259
Syngenta	3.5653	4.8997	-1.0248	-0.6043	0.1789	0.2241	19.12%	0.5534
Zurich	3.0402	9.9509	-4.0551	-0.5641	0.1100	0.2400	21.67%	1.1188

Table 4: Sensitivity to marginal parameter changes. VG model.

Put price:				T = 0.5 $\rho_Y = 0$			
2.0345	(σ,α,μ)	(σ_L,α,μ)	(σ_H,α,μ)	(σ,α_L,μ)	(σ,α_H,μ)	(σ,α,μ_L)	(σ,α,μ_H)
(σ,α,μ)	100.00%						
(σ_L,α,μ)	54.34%	3.28%					
(σ_H,α,μ)	375.34%	334.17%	620.74%				
(σ,α_L,μ)	103.39%	51.17%	372.56%	94.50%			
(σ,α_H,μ)	105.31%	60.23%	386.53%	104.57%	110.88%		
(σ,α,μ_L)	189.25%	145.40%	448.30%	185.59%	196.14%	281.59%	
(σ,α,μ_H)	80.41%	31.72%	363.05%	76.48%	84.02%	172.91%	53.75%

Put price:				T = 1 $\rho_Y = 0$			
6.8241	(σ,α,μ)	(σ_L,α,μ)	(σ_H,α,μ)	(σ,α_L,μ)	(σ,α_H,μ)	(σ,α,μ_L)	(σ,α,μ_H)
(σ,α,μ)	100.00%						
(σ_L,α,μ)	53.14%	5.35%					
(σ_H,α,μ)	250.49%	218.38%	376.15%				
(σ,α_L,μ)	102.69%	57.92%	255.26%	103.12%			
(σ,α_H,μ)	95.72%	50.26%	250.75%	98.79%	91.65%		
(σ,α,μ_L)	140.58%	98.64%	284.49%	141.41%	137.28%	175.17%	
(σ,α,μ_H)	107.30%	65.96%	259.97%	113.40%	105.20%	148.25%	120.99%

Put price:				T = 0.5 $\rho_Y = 0.25$			
1.9730	(σ,α,μ)	(σ_L,α,μ)	(σ_H,α,μ)	(σ,α_L,μ)	(σ,α_H,μ)	(σ,α,μ_L)	(σ,α,μ_H)
(σ,α,μ)	100.00%						
(σ_L,α,μ)	54.98%	2.83%					
(σ_H,α,μ)	373.13%	349.81%	576.90%				
(σ,α_L,μ)	99.72%	51.70%	379.87%	97.94%			
(σ,α_H,μ)	103.63%	56.68%	379.64%	100.12%	106.28%		
(σ,α,μ_L)	182.76%	148.82%	422.09%	184.69%	182.25%	265.01%	
(σ,α,μ_H)	76.62%	31.98%	357.59%	74.33%	83.30%	165.63%	54.75%

Put price:				T = 1 $\rho_Y = 0.25$			
6.0863	(σ,α,μ)	(σ_L,α,μ)	(σ_H,α,μ)	(σ,α_L,μ)	(σ,α_H,μ)	(σ,α,μ_L)	(σ,α,μ_H)
(σ,α,μ)	100.00%						
(σ_L,α,μ)	60.86%	6.21%					
(σ_H,α,μ)	272.94%	243.99%	385.26%				
(σ,α_L,μ)	106.47%	64.67%	273.41%	111.08%			
(σ,α_H,μ)	98.90%	55.99%	267.70%	103.29%	92.66%		
(σ,α,μ_L)	140.66%	110.45%	294.48%	147.81%	137.92%	182.11%	
(σ,α,μ_H)	116.41%	73.02%	277.59%	118.92%	113.98%	152.96%	129.97%

Put price:				T = 0.5 $\rho_Y = 0.75$			
1.6097	(σ,α,μ)	(σ_L,α,μ)	(σ_H,α,μ)	(σ,α_L,μ)	(σ,α_H,μ)	(σ,α,μ_L)	(σ,α,μ_H)
(σ,α,μ)	100.00%						
(σ_L,α,μ)	66.69%	3.60%					
(σ_H,α,μ)	427.57%	422.64%	586.70%				
(σ,α_L,μ)	*100.18%	*61.32%	*436.30%	98.44%			
(σ,α_H,μ)	*110.37%	*73.45%	*426.89%	*122.11%	113.84%		
(σ,α,μ_L)	187.28%	174.55%	459.97%	*209.82%	*199.20%	254.95%	
(σ,α,μ_H)	82.65%	35.15%	421.94%	*77.13%	*92.05%	*189.86%	56.40%

Put price:				T = 1 $\rho_Y = 0.75$			
5.1856	(σ,α,μ)	(σ_L,α,μ)	(σ_H,α,μ)	(σ,α_L,μ)	(σ,α_H,μ)	(σ,α,μ_L)	(σ,α,μ_H)
(σ,α,μ)	100.00%						
(σ_L,α,μ)	66.47%	6.20%					
(σ_H,α,μ)	293.43%	280.18%	379.43%				
(σ,α_L,μ)	*107.59%	*74.25%	*298.61%	108.95%			
(σ,α_H,μ)	*97.83%	*64.56%	*288.90%	*114.62%	89.75%		
(σ,α,μ_L)	135.16%	127.00%	308.76%	*156.31%	*145.55%	173.06%	
(σ,α,μ_H)	113.31%	81.99%	293.19%	*124.94%	*119.06%	*171.56%	128.44%

Marginal Moments				T = 0.5			
	(σ,α,μ)	(σ_L,α,μ)	(σ_H,α,μ)	(σ,α_L,μ)	(σ,α_H,μ)	(σ,α,μ_L)	(σ,α,μ_H)
$Var(Y)$	0.0284	0.0071	0.1134	0.0284	0.0284	0.0403	0.0403
$Skew(Y)$	0.0000	0.0000	0.0000	0.0000	0.0000	-1.2789	1.2789
$Kurt(Y)$	5.2619	5.2619	5.2619	4.1310	7.5238	6.4056	6.4056

Marginal Moments				T = 1			
	(σ,α,μ)	(σ_L,α,μ)	(σ_H,α,μ)	(σ,α_L,μ)	(σ,α_H,μ)	(σ,α,μ_L)	(σ,α,μ_H)
$Var(Y)$	0.0567	0.0142	0.2268	0.0567	0.0567	0.0806	0.0806
$Skew(Y)$	0.0000	0.0000	0.0000	0.0000	0.0000	-0.9043	0.9043
$Kurt(Y)$	4.1310	4.1310	4.1310	3.5655	5.2619	4.7028	4.7028

Marginal parameters: $\{\sigma_L, \sigma, \sigma_H\}$ = $\{0.115, 0.230, 0.460\}$, $\{\alpha_L, \alpha, \alpha_H\}$ = $\{0.188, 0.377, 0.754\}$, $\{\mu_L, \mu, \mu_H\}$ = $\{-0.252, 0, 0.252\}$. * indicates that the correlation level can not be reached. Base put prices are reported at the top left corner of each table. In each column we change one marginal parameter of one process, while in each row we change one marginal parameter of the other process. On the main diagonal, the two marginal distributions are identical. Marginal moments corresponding to different parameter sets are shown at the bottom of the table.

Table 5: Sensitivity to marginal parameter changes. NIG model.

Put price: T = 0.5 $\rho_Y = 0$

2.0356	(γ,β,δ)	(γ_L,β,δ)	(γ_H,β,δ)	(γ,β_L,δ)	(γ,β_H,δ)	(γ,β,δ_L)	(γ,β,δ_H)
(γ,β,δ)	100.00%						
(γ_L,β,δ)	188.16%	269.71%					
(γ_H,β,δ)	56.42%	143.31%	17.34%				
(γ,β_L,δ)	145.78%	225.28%	99.61%	194.38%			
(γ,β_H,δ)	81.46%	170.89%	42.26%	132.98%	71.31%		
(γ,β,δ_L)	64.27%	150.40%	24.66%	109.99%	52.19%	29.04%	
(γ,β,δ_H)	208.78%	285.65%	173.43%	254.49%	198.17%	179.41%	311.18%

Put price: T = 1 $\rho_Y = 0$

6.5146	(γ,β,δ)	(γ_L,β,δ)	(γ_H,β,δ)	(γ,β_L,δ)	(γ,β_H,δ)	(γ,β,δ_L)	(γ,β,δ_H)
(γ,β,δ)	100.00%						
(γ_L,β,δ)	149.97%	205.14%					
(γ_H,β,δ)	64.38%	122.64%	27.73%				
(γ,β_L,δ)	117.43%	177.87%	86.02%	140.51%			
(γ,β_H,δ)	100.37%	158.16%	65.78%	121.92%	102.42%		
(γ,β,δ_L)	64.75%	125.55%	30.04%	86.63%	66.30%	30.56%	
(γ,β,δ_H)	169.43%	220.00%	144.28%	191.18%	173.07%	143.49%	236.56%

Put price: T = 0.5 $\rho_Y = 0.25$

1.8406	(γ,β,δ)	(γ_L,β,δ)	(γ_H,β,δ)	(γ,β_L,δ)	(γ,β_H,δ)	(γ,β,δ_L)	(γ,β,δ_H)
(γ,β,δ)	100.00%						
(γ_L,β,δ)	196.75%	271.40%					
(γ_H,β,δ)	61.22%	157.71%	17.77%				
(γ,β_L,δ)	146.64%	236.04%	108.04%	188.68%			
(γ,β_H,δ)	92.82%	177.46%	50.33%	132.88%	73.15%		
(γ,β,δ_L)	63.98%	162.27%	24.67%	118.44%	56.22%	33.30%	
(γ,β,δ_H)	215.83%	303.89%	188.98%	257.50%	207.85%	188.19%	325.53%

Put price: T = 1 $\rho_Y = 0.25$

5.8367	(γ,β,δ)	(γ_L,β,δ)	(γ_H,β,δ)	(γ,β_L,δ)	(γ,β_H,δ)	(γ,β,δ_L)	(γ,β,δ_H)
(γ,β,δ)	100.00%						
(γ_L,β,δ)	160.05%	208.01%					
(γ_H,β,δ)	67.51%	132.20%	30.50%				
(γ,β_L,δ)	122.32%	177.40%	93.11%	145.26%			
(γ,β_H,δ)	104.75%	164.02%	74.60%	124.42%	112.21%		
(γ,β,δ_L)	68.43%	133.61%	31.30%	93.06%	74.44%	30.98%	
(γ,β,δ_H)	179.98%	230.71%	154.59%	196.11%	184.00%	153.66%	242.81%

Put price: T = 0.5 $\rho_Y = 0.75$

1.5166	(γ,β,δ)	(γ_L,β,δ)	(γ_H,β,δ)	(γ,β_L,δ)	(γ,β_H,δ)	(γ,β,δ_L)	(γ,β,δ_H)
(γ,β,δ)	100.00%						
(γ_L,β,δ)	*68.01%	270.20%					
(γ_H,β,δ)	*12.15%	*11.94%	17.44%				
(γ,β_L,δ)	142.99%	*128.89%	11.44%	186.98%			
(γ,β_H,δ)	90.59%	*46.35%	*10.18%	135.38%	76.09%		
(γ,β,δ_L)	*67.75%	188.90%	*11.75%	*132.24%	*48.26%	30.50%	
(γ,β,δ_H)	*209.19%	*216.71%	221.84%	*220.71%	*224.16%	*209.07%	330.53%

Put price: T = 1 $\rho_Y = 0.75$

4.8473	(γ,β,δ)	(γ_L,β,δ)	(γ_H,β,δ)	(γ,β_L,δ)	(γ,β_H,δ)	(γ,β,δ_L)	(γ,β,δ_H)
(γ,β,δ)	100.00%						
(γ_L,β,δ)	*66.36%	207.65%					
(γ_H,β,δ)	*19.00%	*18.45%	28.54%				
(γ,β_L,δ)	120.82%	*100.56%	19.35%	140.84%			
(γ,β_H,δ)	104.39%	*70.95%	19.24%	122.04%	111.52%		
(γ,β,δ_L)	*68.94%	148.81%	*19.38%	*101.56%	*71.38%	31.24%	
(γ,β,δ_H)	*172.06%	*173.55%	177.34%	*171.11%	*172.43%	*171.19%	240.77%

Marginal Moments T = 0.5

	(γ,β,δ)	(γ_L,β,δ)	(γ_H,β,δ)	(γ,β_L,δ)	(γ,β_H,δ)	(γ,β,δ_L)	(γ,β,δ_H)
$Var(Y)$	0.0264	0.0529	0.0132	0.0321	0.0321	0.0132	0.0529
$Skew(Y)$	0.0000	0.0000	0.0000	-0.9322	0.9322	0.0000	0.0000
$Kurt(Y)$	5.2200	7.4400	4.1100	6.5283	6.5283	7.4400	4.1100

Marginal Moments T = 1

	(γ,β,δ)	(γ_L,β,δ)	(γ_H,β,δ)	(γ,β_L,δ)	(γ,β_H,δ)	(γ,β,δ_L)	(γ,β,δ_H)
$Var(Y)$	0.0529	0.1057	0.0264	0.0643	0.0643	0.0264	0.1057
$Skew(Y)$	0.0000	0.0000	0.0000	-0.6592	0.6592	0.0000	0.0000
$Kurt(Y)$	4.1100	5.2200	3.5550	4.7642	4.7642	5.2200	3.5550

Marginal parameters used in the sensitivity analysis: $\{\gamma_L, \gamma, \gamma_H\}$ = $\{3.575, 7.150, 14.300\}$, $\{\beta_L, \beta, \beta_H\}$ = $\{-2.500, 0.000, 2.500\}$, $\{\delta_L, \delta, \delta_H\}$ = $\{0.189, 0.378, 0.756\}$. * indicates that the correlation level can not be reached. Base put prices are reported at the top left corner of each table. In each column we change one marginal parameter of one process, while in each row we change one marginal parameter of the other process. On the main diagonal, the two marginal distributions are identical. Marginal moments corresponding to different parameter sets are shown at the bottom of the table.

(a) 6-months, $\rho_Y = 0$ (b) 1-year, $\rho_Y = 0$

(c) 6-months, $\rho_Y = 0.25$ (d) 1-year, $\rho_Y = 0.25$

(e) 6-months, $\rho_Y = 0.75$ (f) 1-year, $\rho_Y = 0.75$
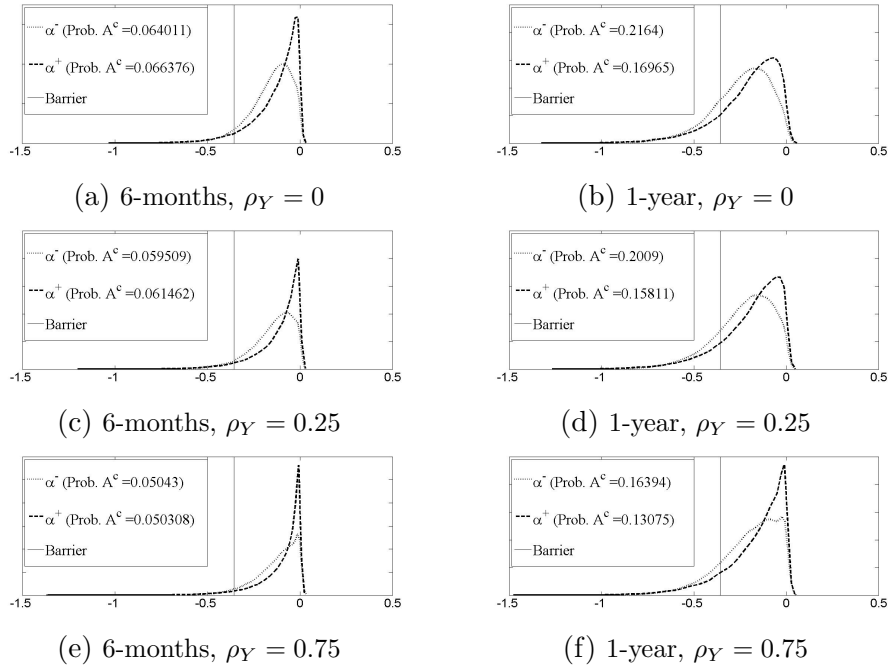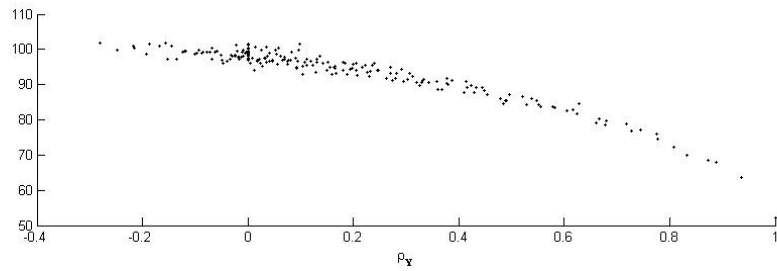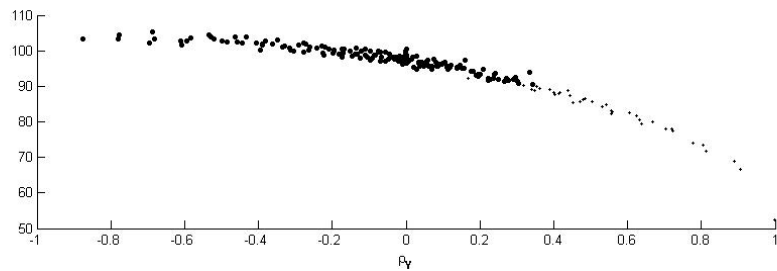
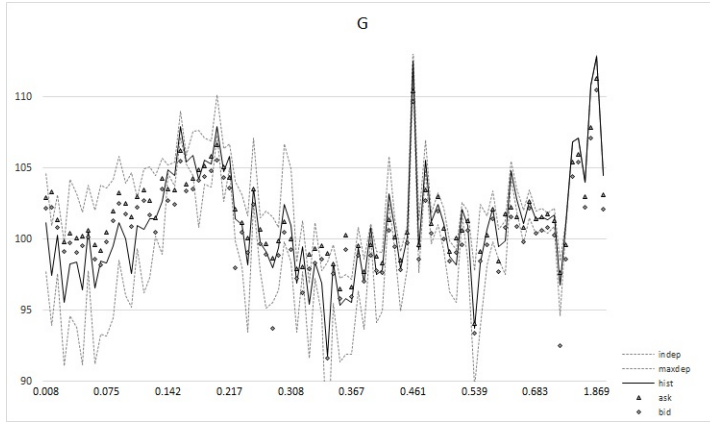Figure 2: Distribution of the minimum of log-returns at maturity. VG model.
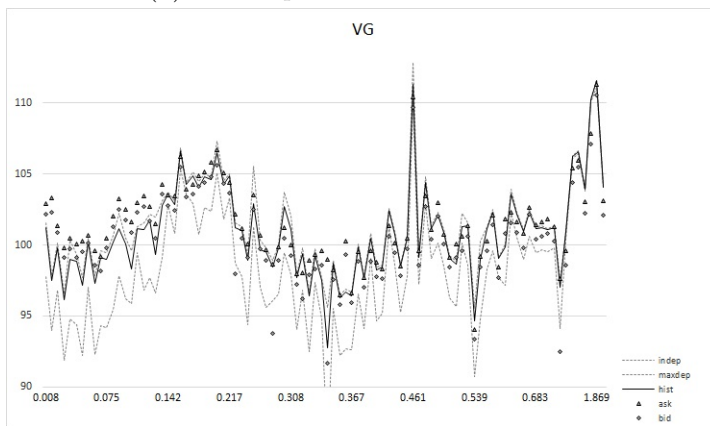

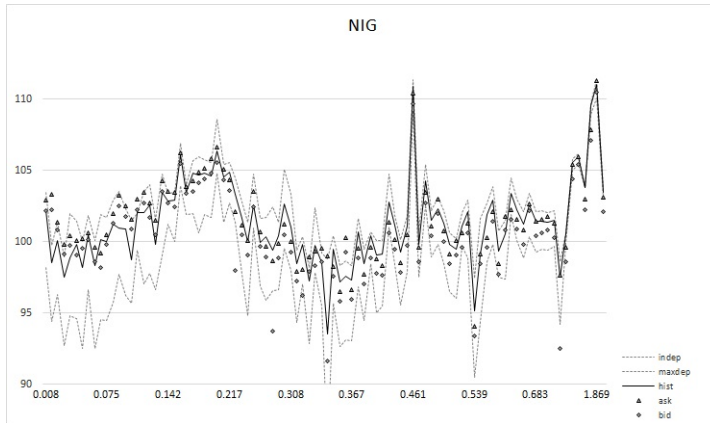(a) Put prices under the VG model

(b) Put prices under the NIG model

Figure 3: Sensitivity to correlation changes.

(a) MBRC prices under the G model

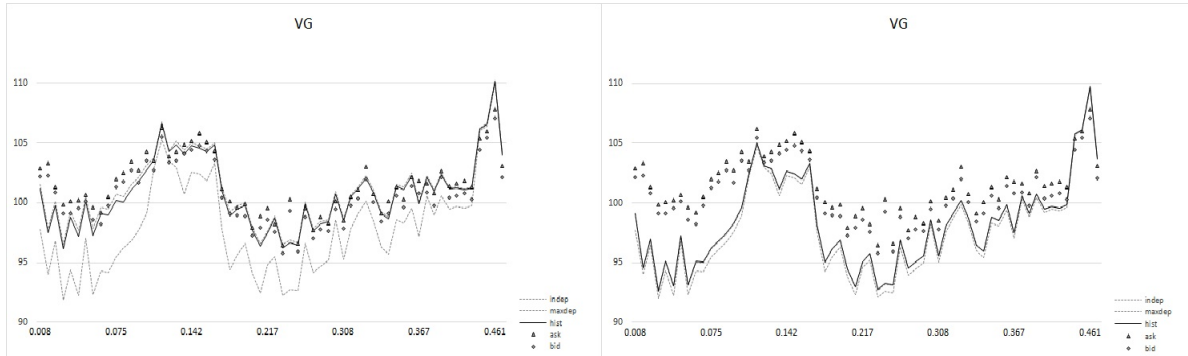(b) MBRC prices under the VG model
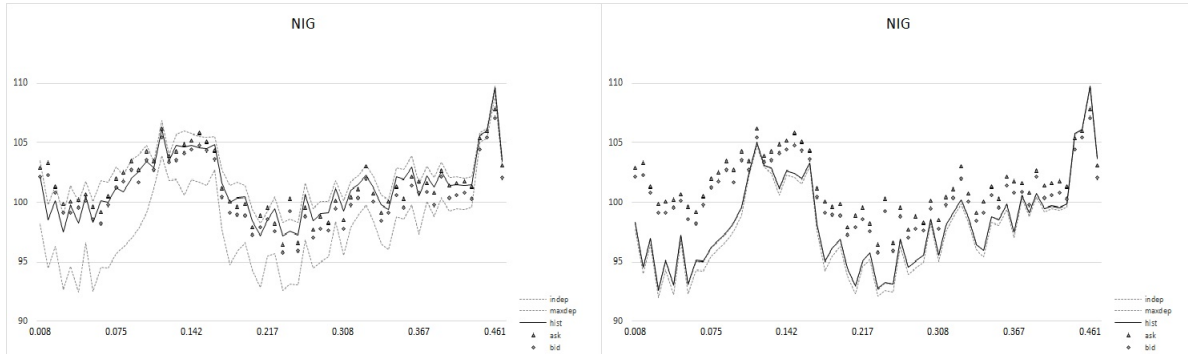

(c) MBRC prices under the NIG model

Figure 4: MBRC prices (full dataset). Joint calibration. Observed bid and ask prices are represented by squares and triangles, respectively. Solid line represents model prices, with common parameters calibrated to historical correlations. Dashed lines are model prices with with common parameters set to reproduce maximum pairwise correlations (upper dashed line) and independence between marginal processes (lower dashed line). MBRCs are ordered depending on the time to issue, indicated on the horizontal axis of each graph.
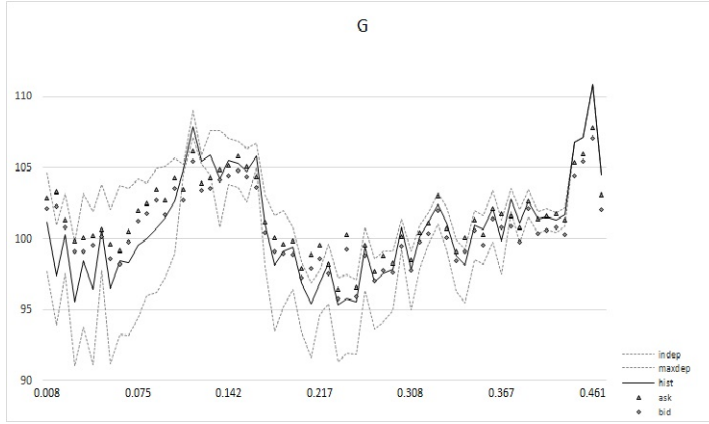
(a) MBRC prices under the G model.

(b) MBRC prices under the VG model. Joint calibration (left) and two-step calibration (right).

(c) MBRC prices under the NIG model. Joint calibration (left) and two-step calibration (right).

Figure 5: MBRC prices on Nestlé, Novartis, RocheGS only. Parameters: $\boldsymbol{\sigma}_G = \{0.1522, 0.1872, 0.1892\}$; $\boldsymbol{\sigma}_{VG}^{(Joint)} = \{0.1338, 0.1142, 0.1080\}$, $\boldsymbol{\alpha}_{VG}^{(Joint)} = \{0.4181, 0.3142, 0.1985\}$, $\boldsymbol{\mu}_{VG}^{(Joint)} = \{-0.1263, -0.2508, -0.3321\}$, $a_{VG}^{(Joint)} = 2.3918$, $\boldsymbol{\rho}_{VG}^{(Joint)} = \{0.7178, 0.6063, 0.5899\}$; $\boldsymbol{\gamma}_{NIG}^{(Joint)} = \{3.6748, 3.6708, 3.6650\}$, $\boldsymbol{\beta}_{NIG}^{(Joint)} = \{-0.7746, -0.8606, -0.7193\}$, $\boldsymbol{\delta}_{NIG}^{(Joint)} = \{0.1079, 0.1367, 0.1509\}$, $a_{NIG}^{(Joint)} = 2.3918$, $\boldsymbol{\rho}_{NIG}^{(Joint)} = \{0.7124, 0.6124, 0.6899\}$.

References

Guillaume, F. (2012). The αvg model for multivariate asset pricing: calibration and extension. *Review of Derivatives Research*, 16(1):25–52.

Jackson, K. R., Jaimungal, S., and Surkov, V. (2008). Fourier space time-stepping for option pricing with lévy models. *Journal of Computational Finance*, 12(2):1–29.

Leoni, P. and Schoutens, W. (2008). Multivariate smiling. *Wilmott Magazine*.

Lindauer, T. and Seiz, R. (2008). Pricing (multi-) barrier reverse convertibles. *Available at SSRN 1160297*.

Luciano, E., Marena, M., and Semeraro, P. (2013). Dependence calibration and portfolio fit with factor-based time changes. *Carlo Alberto Notebooks*, (307).

Luciano, E. and Schoutens, W. (2006). A multivariate jump-driven financial asset model. *Quantitative finance*, 6(5):385–402.

Luciano, E. and Semeraro, P. (2010). Multivariate time changes for lévy asset models: Characterization and calibration. *Journal of Computational and Applied Mathematics*, 233(8):1937–1953.

Madan, D. B. and Seneta, E. (1990). The variance gamma (vg) model for share market returns. *Journal of business*, pages 511–524.

Semeraro, P. (2008). A multivariate variance gamma model for financial applications. *International journal of theoretical and applied finance*, 11(01):1–18.

Wallmeier, M. and Diethelm, M. (2008). Market pricing of exotic structured products: The case of multi-asset barrier reverse convertibles in switzerland. *Available at SSRN 1095772*.

Wallmeier, M. and Diethelm, M. (2012). Multivariate downside risk: Normal versus variance gamma. *Journal of Futures Markets*, 32(5):431–458.